RSC Advances

PAPER

View Article Online
View Journal | View Issue

Cite this: *RSC Adv.*, 2018, **8**, 29044

Influence of residual sodium ions on the structure and properties of poly(3,4-ethylenedioxythiophene):poly(styrenesulfonate)†

Hangyeol Cho, Wonseok Cho, Youngno Kim, Jin-geun Lee and Jung Hyun Kim *

Received 15th June 2018
Accepted 5th August 2018

DOI: 10.1039/c8ra05150j

rsc.li/rsc-advances

Poly(3,4-ethylenedioxythiophene):poly(styrenesulfonate) (PEDOT:PSS) is a promising conducting polymer in terms of its applicability to transparent and flexible electronic devices. Generally, a negatively charged PSS chain can interact with alkali metal cations like sodium and potassium. During polymerization, these ions, especially sodium ions, remain in an aqueous state and affect particle formation. This paper describes the effect of residual sodium ions on the synthesis of PEDOT:PSS and its electrical and optical properties. Removing the sodium ions weakens the coulombic interaction between the PEDOT and PSS chains, which leads to a linear conformation. This conformational change enhances the electrical conductivity and work function. Furthermore, transmittance in the visible region increased remarkably because the intrinsic electrical properties of the PEDOT:PSS particles were improved. Moreover, the colloidal stability was enhanced because the particle coagulation caused by residual sodium ions was reduced. In summary, we determined that sodium ions in PEDOT:PSS have a considerable influence on its electrical and optical properties and colloidal stability for practical applications.

Introduction

Conducting polymers have been studied and developed as promising materials for organic devices. This is because they have the properties of both metals, such as highly conductive doped states, and polymers, such as optical transparency and flexibility.[1–4]

Among the conducting polymers, poly(3,4-ethylenedioxythiophene):poly(styrenesulfonate), also known as PEDOT:PSS, is the most widely used material because of its high electrical conductivity, low band gap, and transparency in the visible region compared to those of others.[5–7] While most conducting polymers tend to be insoluble in any solvent, PEDOT:PSS can be dispersed in water and some polar organic solvents in the form of colloidal particles. This is because hydrophilic PSS acts as a charge-balancing counter-ion to stabilize hydrophobic PEDOT.[8,9]

These advantages of PEDOT:PSS enable the application of solution processing technology and the replacement of inorganic materials with organic light-emitting diodes (OLEDs) and organic photovoltaic cells (OPVs).[10,11] In these organic devices, PEDOT:PSS is commonly used as a hole-transporting layer (HTL) because it has relatively high hole mobility for the alignment of the work function of interfacial layers between the electrode and active layer.[12] Because this decrease in the energy barrier at the electrode contacts improves device performance, applications using PEDOT:PSS as a hole-transporting material have been developed.

PEDOT:PSS is synthesized through the oxidation polymerization of 3,4-ethylenedioxythiophene (EDOT) into PSS chains dispersed in water. The positive charges of PEDOT chains combine with the negative charges of PSS chains *via* a coulombic interaction.[13] This negative charge of PSS chains can combine with metal ions like sodium and potassium. In previous studies, the metal ions had a significant impact on the properties of PEDOT:PSS and its application. Weijtens *et al.* investigated the effect of the alkali metal content on the electronic properties of PEDOT:PSS by adding NaOH and CsOH.[14] In applications to the buffer layer of devices like OLEDs and OPVs, the sodium ions in PEDOT:PSS are known to have a significant impact on the lifetime of the devices owing to the penetration of the sodium ions into the contact layer.[15] Generally, PSS exists in the form of poly(sodium-4-styrenesulfonate) (PSSNa). This is because poly(4-styrenesulfonic acid) (PSSH) is so unstable that it usually exists in salt form. For this reason, during synthesis, the residual sodium ions from PSS are present. These ions have a dominating influence on the structure of PEDOT:PSS particles during polymerization and may lead to different properties.

Therefore, in this work, we focus on the effect of the difference between acid and metal ions on the synthesis, electrical and optical properties, and colloidal stability of PEDOT:PSS particles. The electrical and optical properties are important for

Department of Chemical and Biomolecular Engineering, Yonsei University, 50 Yonsei-ro, Seodaemoon-Gu, Seoul, 03722, South Korea. E-mail: Jayhkim@yonsei.ac.kr; Fax: +82 2 312 0305; Tel: +82 2 2123 4693

† Electronic supplementary information (ESI) available. See DOI: 10.1039/c8ra05150j

applications to electronic devices, and colloidal stability is important for processability. We synthesized sodium-removed PEDOT:PSS dispersions using PSSH and sodium-containing PEDOT:PSS dispersions using PSSNa. For the HTL, a PEDOT-to-PSS ratio of 1 : 6 was selected. Then, we compared the sodium ion concentrations and the structural and morphological changes in the PEDOT:PSS particles. We also examined their electrical properties, such as their conductivity and work function, and optical properties, such as their transmittance, b*, and haziness. Through viscosity changes over time, the colloidal stabilities of the PEDOT:PSS solutions with and without sodium ions were compared. We consider that we can improve the applicability of organic electronic devices by studying the effects of residual sodium ions on the characteristics of PEDOT:PSS.

Experimental

Materials

EDOT (97%), poly(4-styrenesulfonic acid) (PSS), iron(III) sulfate hydrate ($Fe_2(SO_4)_3$; 97%), sodium persulfate ($Na_2S_2O_8$; 98%), and dimethyl sulfoxide (DMSO; 98%) were purchased from Sigma-Aldrich. The ion exchange resin was purchased from Samyang Co.

Fabrication of sodium-containing and sodium-removed PEDOT:PSS

The polymerizations of sodium-containing and sodium-removed PEDOT:PSS were performed using PSSNa and PSSH, respectively, and EDOT, $Fe_2(SO_4)_3$, and $Na_2S_2O_8$ were used for both. The reaction temperature was 10 °C and the conditions were kept constant for 24 h under an argon atmosphere. The synthesis followed the Baytron P procedure[16] and the ratio of PEDOT to PSS was 1 : 6. Sodium-removed PEDOT:PSS was synthesized using a PSSH solution that had undergone the following ion exchange process. A 1 M PSSNa solution and cationic ion exchange resin of equal volume were prepared. Using a column, ion exchange was performed at 25 °C and atmospheric pressure. Sodium-containing PEDOT:PSS was synthesized using PSSNa without the above-mentioned process. All of the PEDOT:PSS films used in the analysis were fabricated by spin coating for 30 s and then annealing at 150 °C for 2 min. The thickness of the film was approximately 100 nm. DMSO was added to the PEDOT:PSS dispersions at 5 wt% as needed.

Characterization

To measure the sodium ion concentration in PEDOT:PSS, inductively coupled plasma-optical emission spectrometry (ICP-OES; Optima 8300, PerkinElmer) and scanning electron microscopy with energy dispersive X-ray spectroscopy (SEM-EDS; JEOL-7800F, JEOL Ltd.) were used. The structures were examined using X-ray photoelectron spectroscopy (XPS; Thermo UK, K-alpha) using monochromated Al Kα X-ray radiation and Raman spectroscopy (LabRam Aramis, Horiba Jobin Yvon) using a 633 nm He–Ne laser as the excitation source. The morphologies of thin films were examined using atomic force microscopy (AFM; XE-100, Park Systems) with topographic and phase images. The electrical properties, namely conductivity and work function, were examined with and without DMSO. In the case of DMSO addition, 5 wt% of the PEDOT:PSS dispersion was added. The sheet resistance was measured using the four-point probe method (RT-70/RG-5, Napson), and the thickness

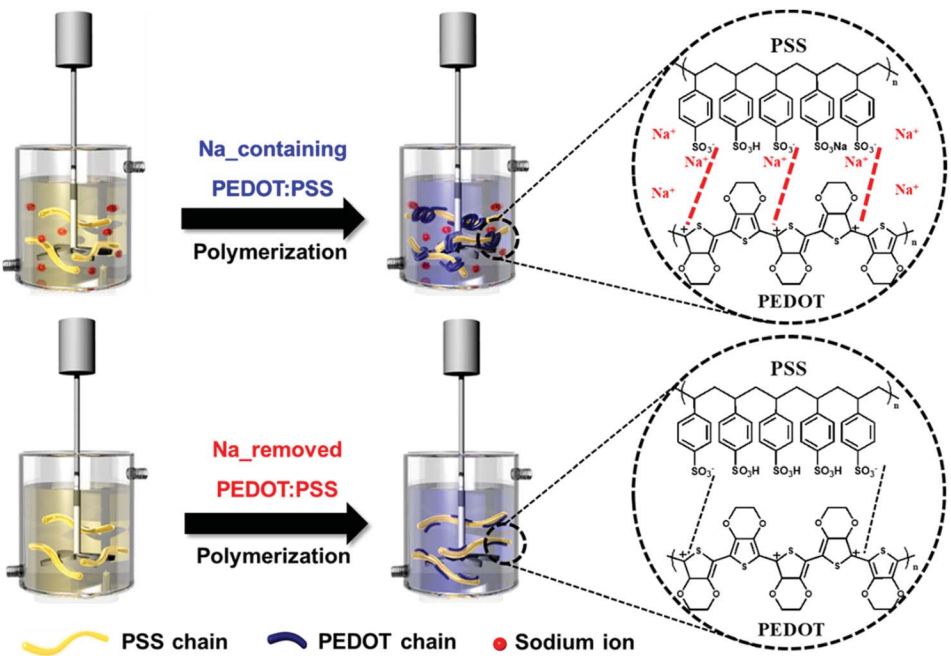

Fig. 1 Schematic of synthesis of PEDOT:PSS with and without sodium ions. The chemical structures show the interaction between the PEDOT and PSS chains.

of the film was measured using a surface profiler (DektakXT Stylus Profiler, Bruker). The work function was obtained through UV photoelectron spectroscopy (UPS; PHI 5000 Versa Probe II, Ulvac-PHI) of thin films on indium tin oxide (ITO) substrates. Transmittance, haziness, and L*a*b* color at 550 nm were measured using a haze and color meter (COH 400, Nippon Denshoku). Film samples with various sheet resistances were spin coated on glass substrates with 91% visible light transmittance. To analyze colloidal stability, viscosity changes were observed for 90 days. The viscosity was measured using a viscometer (LVDV-II+, Brookfield, 25 °C).

Results and discussion

Analysis of sodium ion content

During the synthesis of PEDOT:PSS with residual sodium ions, PSS exists in three forms: poly(styrenesulfonate anion) (PSS^-), which interacts with the positive charge of PEDOT, poly(styrenesulfonic acid) (PSSH), and its sodium salt (PSSNa).[14] These PSS forms determine the conformational structure of PEDOT:PSS particles. In the case of PEDOT:PSS containing sodium ions, a relatively large amount of PSSNa exists in the PSS chains. PSSNa tends to ionize in water; some sulfonate groups are present in the PSS^- form, where the negative charge is placed. These negative charges can interact with the positive charges of PEDOT through coulombic attraction,[17] leading to the coiled conformation. While sodium-removed PEDOT:PSS has linear and expanded-coil conformation (Fig. 1).

To confirm this structural change, we synthesized Na-containing and Na-removed PEDOT:PSS using PSSNa and PSSH, respectively. First, we detected a decrease in the amount of sodium ions in both the dispersion and the film. ICP analysis and ion conductivity were used to confirm the decrease in sodium ion concentration in the dispersion. Fig. 2(a) shows that the ion conductivity decreased from 168.7 to 62.0 mS. A reduction in sodium ion concentration in the dispersion from 56 to 23 ppm was observed through ICP analysis. In order to determine whether sodium ions influence the composition of a PEDOT:PSS film surface, SEM-EDS analyses were conducted. Comparison of the SEM micrograph and EDS analysis results of the PEDOT:PSS film displayed in Fig. S1† revealed that the weight percentage of C was almost identical, which means that the amount of PEDOT:PSS on the surface was approximately equal.[18,19] On the other hand, the weight percentage of Na in the PEDOT:PSS film decreased significantly from 3.28% to almost 0%. Similarly, it was found that the Na (1s) peak from XPS analysis was also substantially smaller (Fig. 2(b)). These results show a greater decrease than the ICP analysis which conducts under dispersion condition. This is because the hydrophilic PSS rich layer is located on the upper part of the film after annealing, so it is difficult to detect the low sodium ion concentration on the surface.

Structural and morphological changes of PEDOT:PSS particles

The surface chemical compositions of the PEDOT:PSS films with and without sodium ions were analyzed using XPS. The S (2p) and O (1s) peaks were deconvoluted according to the work of Greczynski *et al.*[20,21] to obtain the separate peaks of PSSNa and PSSH. The S (2p) spectra for Na-containing and removed PEDOT:PSS films are shown respectively in Fig. 2(c) and (d). Because the sulfur atoms from PEDOT and PSS have different chemical bonds, the S (2p) bands have different binding

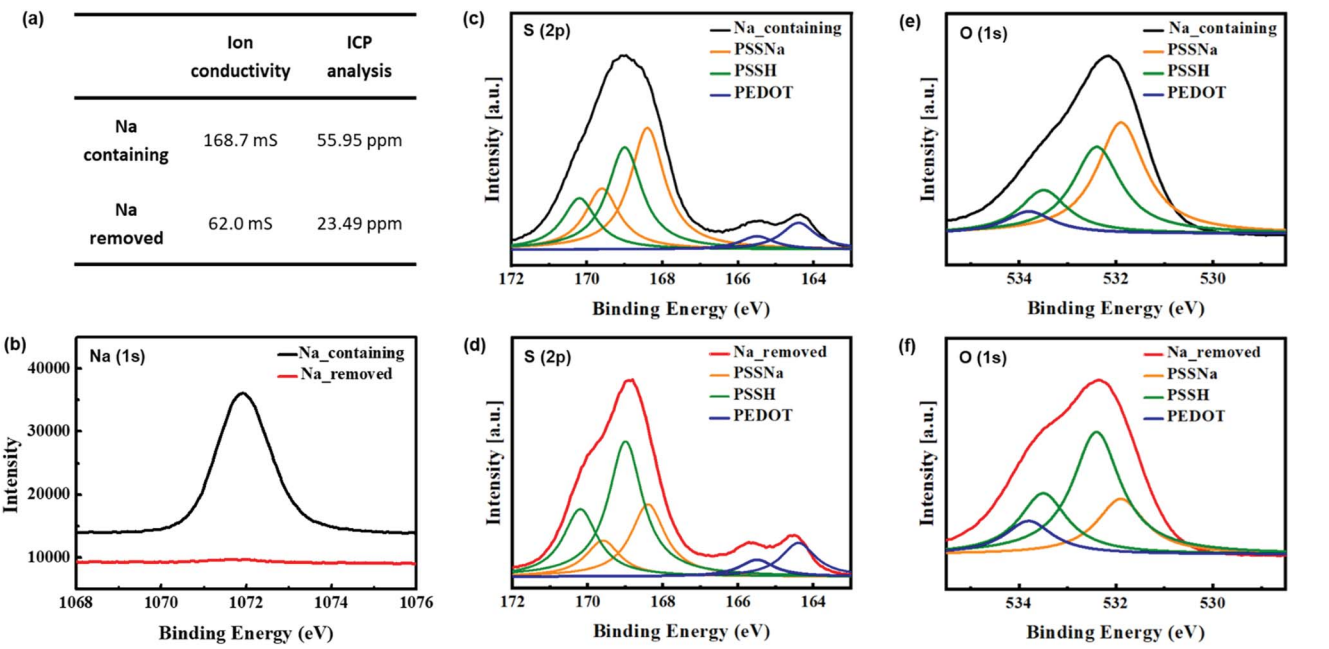

Fig. 2 (a) Ion conductivity and ICP analysis results of Na-containing and removed PEDOT:PSS dispersions, (b) Na (1s), (c) and (d) S (2p), (e) and (f) O (1s) XPS spectra of Na-containing and removed PEDOT:PSS. The XPS spectra were normalized to the PSS contribution (hydrocarbon calibration to 285 eV).

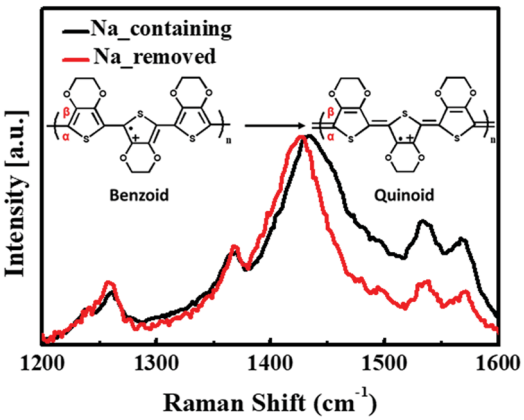

Fig. 3 Raman spectra of PEDOT:PSS films (under 632.8 nm He–Ne laser excitation). Inset image shows change from benzoid to quinoid structure resulting in peak reduction (1400–1600 cm^{-1}).

energies. The lower binding energy peaks, at 164.4 and 165.5 eV, are consistent with the S ($2p_{3/2}$) and S ($2p_{1/2}$) sulfur atoms in PEDOT (blue), and the higher binding energy peaks at approximately 169 eV are consistent with the sulfur atoms in the sulfonate groups of PSS.[16,22,23] This peak is deconvoluted into two binding energy peaks of PSSNa and PSSH. The lower binding energy peaks at 168.4 and 169.6 eV are associated with the S ($2p_{3/2}$) and S ($2p_{1/2}$) sulfur atoms in PSSNa (yellow), and the higher binding energy peaks at 169 and 170.2 eV correspond to the S ($2p_{3/2}$) and S ($2p_{1/2}$) sulfur atoms in PSSH (green).[20–22] Comparing these spectra, Na-containing PEDOT:PSS shows that the peaks of PSSNa have a larger area, while Na-removed PEDOT:PSS has a larger area of the peaks of PSSH. This is the result of conversion from PSSNa to by removing sodium ions. Because PSSH has a higher binding energy peak than PSSNa does, it causes the PSS part to shift towards a higher binding energy.[20] Fig. 2(e) and (f) shows the O (1s) spectra deconvoluting three different binding energy peaks of PEDOT, PSSNa and PSSH. Unlike the sulfur atoms, only PSSH is decomposed into two peaks corresponding to S ($2p_{3/2}$) and S ($2p_{1/2}$) spectra (*i.e.* 532.4 and 533.5 eV). The higher peak at 533.8 eV is associated with the oxygen atoms in PEDOT, and the lower peak at 531.9 eV is consistent with the PSSNa.[20–22] As in the case with sulfur atoms, either the conversion from PSSNa to PSSH and the overall peak shifted upward can also be seen.

The conformational changes of the PEDOT chains in the PEDOT:PSS films with and without sodium ions were investigated using Raman spectroscopy (Fig. 3). The peaks at 1530, 1440, 1370, and 1270 cm^{-1} corresponded to the asymmetric $C_\alpha = C_\beta$, symmetric $C_\alpha = C_\beta$, C_β–C_β stretching, and C_α–C_α inter-ring stretching vibration modes of the five-membered rings of PEDOT, respectively.[24–26] The intensity of peak bands at 1400–1600 cm^{-1}, which consists of the degree of localization of holes, was reduced. It suggests that the changes from dedoped (benzoid) to doped-state (quinoid) of PEDOT chains by removing the sodium ions.[27,28] This result indicates that the residual sodium ions affect the doping site of PEDOT, and are in good agreement with data by M. M. de Kok *et al.*[27] In addition, this decreased intensity is similar to that of the PEDOT:PSS treated using organic solvents such as EG[29–31] or acid[32] which reduce the interaction between the PEDOT and PSS chains.[13] These results indicate that Na-containing PEDOT:PSS has the stronger interaction between the two chains than Na-removed PEDOT:PSS. This is because the lower electronegativity of sodium compared to hydrogen results in the excess of PSS anions by ionization of the PSSNa in water. While polymerization of PEDOT:PSS, these negative charges affect the coulombic interaction between PEDOT and PSS chains.[14] Thus, the reduced interaction after the removal of sodium ions causes the conformational change from coil to linear or expanded-coil structure, which should delocalize the conjugate π-electron.

To confirm the morphological changes of the PEDOT:PSS particles, AFM images were analyzed. Generally, the DMSO

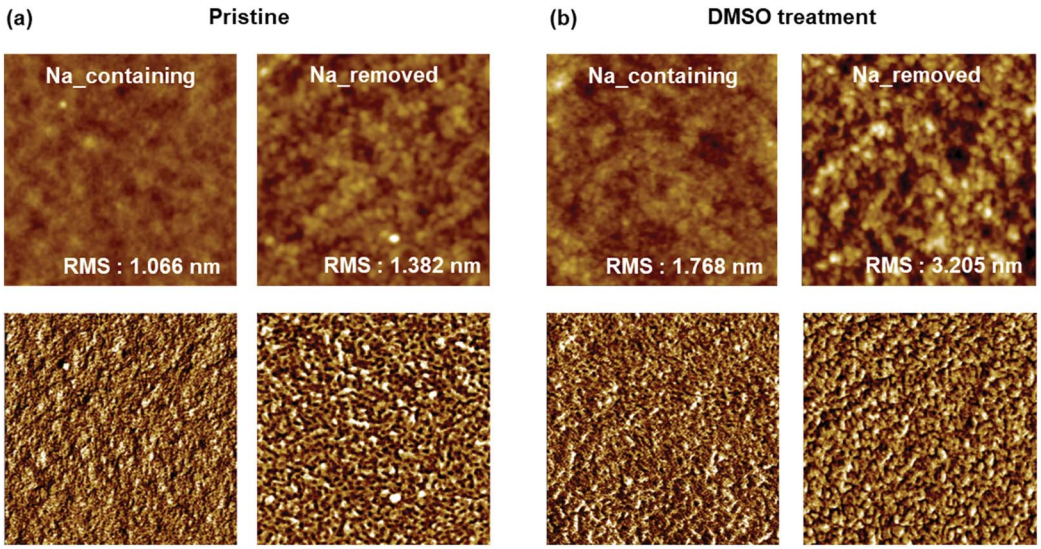

Fig. 4 AFM topographic (upper) and phase (bottom) images of PEDOT:PSS films: (a) pristine and (b) with 5% DMSO solution treatment. All images are 2 × 2 μm.

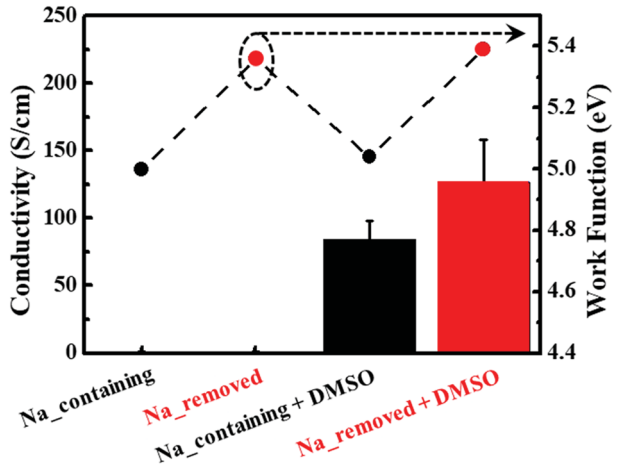

Fig. 5 Electrical conductivities (bar) and work functions (dot) of PEDOT:PSS films with and without 5% DMSO solution treatment. The error bars represent the standard deviation from several measurements.

solution treatment increased the conductivity of the PEDOT:PSS films through phase separation between PEDOT and PSS.[13]

In this study, we compared the morphologies of PEDOT:PSS films before and after DMSO treatment; sodium ions were retained or removed during polymerization. In the AFM topographic and phase images (Fig. 4), there are bright and dark phase shifts corresponding to PEDOT-rich and PSS-rich grains on the film surface.[33–35] Without DMSO treatment, the separation between two grains was unclear and the surface was smooth. On the other hand, with DMSO treatment, PEDOT grains expanded and the roughness increased. In the case of Na-removed PEDOT:PSS, the root-mean-square (rms) roughness increased significantly from 1.382 to 3.205 nm with DMSO addition. In contrast, a slight increase from 1.066 to 1.768 nm was observed in the case of Na-containing PEDOT:PSS. The results show that the residual sodium ions prevent PEDOT grains from expanding by interfering with the phase separation caused by DMSO treatment.

Electrical and optical properties of PEDOT:PSS with and without sodium ions

As the structures of the PEDOT:PSS particles have a significant impact on their properties, we investigated the electrical and optical properties. The electrical conductivities of sodium-containing and sodium-removed PEDOT:PSS are shown in Fig. 5 (left axis). The electrical conductivity of PEDOT:PSS can be determined from the product of carrier concentration and carrier mobility.[36,37] It is widely demonstrated that the mechanism for the electrical properties enhancements of PEDOT:PSS is owing to the phase separation by decreasing the interaction between PEDOT and PSS chains. This is because that the phase separation causes partial reorientation of PEDOT chains and reduces the distance between PEDOT grains. So that the carriers in the PEDOT chains can better hop into other chains, improving its mobility.[13,38] As mentioned in previous Raman

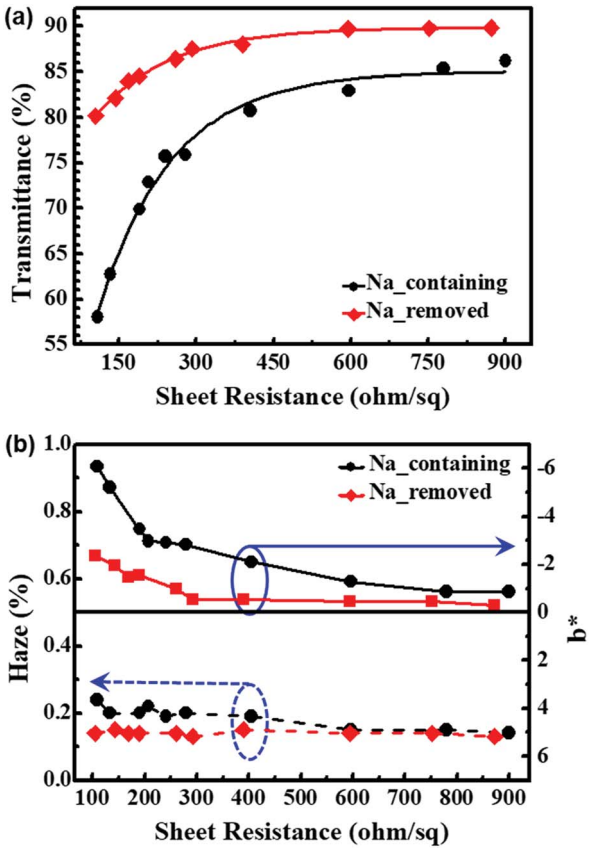

Fig. 6 Variations in (a) transmittance and (b) haziness (left) and b* (right) of PEDOT:PSS films treated with 5% DMSO solution with respect to sheet resistance.

results, in the case of PEDOT:PSS for which sodium ions were removed during polymerization, the doping level of PEDOT chains increased. Also, the interaction between PEDOT and PSS chains decreased due to the lower electronegativity of sodium ions combined with the sulfonate groups of PSS chains. This occurred the phase separation of PEDOT:PSS, leading to the conformational change from a coil to a linear structure and the extension of PEDOT grains. This makes it possible for the carriers in PEDOT chains to hop more effectively to other chains, enhancing conductivity by increasing carrier mobility.[36] As a result, PEDOT:PSS without sodium ions was almost twice as conductive (approximately 130 S cm^{-1}) as PEDOT:PSS with sodium ions (70 S cm^{-1}). Without DMSO, the conductivities of both were lower than 1 S cm^{-1} because there was no phase separation effect from the addition of organic solvents, such as DMSO, DMF, or THF.

The work function values and their corresponding UPS spectra for sodium-containing and sodium-removed PEDOT:PSS are also shown in Fig. 5 (right axis) and S2.† Based on the UPS spectra, the work functions could be calculated from the following equation:[39]

$$\text{Work function } (\Phi) = h\nu - |E_{\text{cutoff}} - E_{\text{F}}|$$

where $h\nu$ = 21.21 eV is the energy of the UV photons for He I radiation and the E_{cutoff} is the binding energy of the secondary

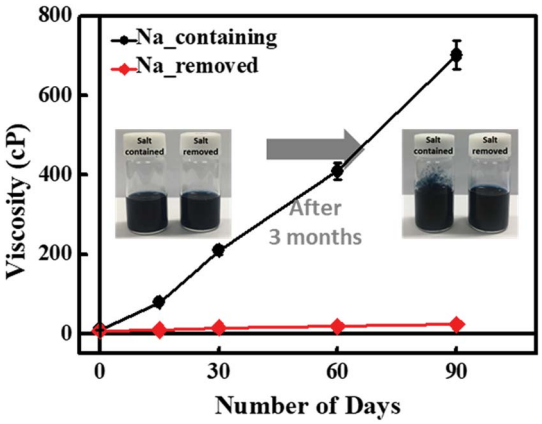

Fig. 7 Variations in viscosity of PEDOT:PSS dispersions with respect to time. The error bars represent the standard deviation from several measurements. Inset images show Na-containing and Na-removed PEDOT:PSS dispersions immediately after synthesis and after three months.

edge. The Fermi energy (E_F) was located at 0 eV. When DMSO was added, the work functions were approximately equal to those of pristine samples. However, the work function of PEDOT:PSS was increased significantly from 5.04 to 5.39 eV by removing sodium ions during polymerization. This is because hydrogen is more electronegative than sodium, so the binding energy of PSSH is higher than that of PSSNa.[14] For this reason, PSSNa tends to exist in water as Na^+ and PSS^-, which increases the electron density of PSSNa so that it has a higher Fermi level. As a result, the work function of PSSH is higher than that of PSSNa.[40]

The optical properties of PEDOT:PSS in the visible region are very important for applications to transparent electronic devices. In this study, we analyzed the transmittance, haziness, and L*a*b* color at 550 nm of PEDOT:PSS films synthesized with and without sodium ions. Because PEDOT:PSS is blue, only the b* value is discussed. The absolute value of b* represents the intensity of the blue color: higher the value of b*, the more blue is PEDOT:PSS. The films were prepared to have various sheet resistances between 150 and 1000 $\Omega\ \square^{-1}$, corresponding to film thicknesses between 500 and 100 nm.

Fig. 6(a) shows that both Na-containing and Na-removed PEDOT:PSS films saw a reduction in transmittance as sheet resistance decreased. Overall, Na-removed PEDOT:PSS films showed better transmittance, and there were large differences when the sheet resistance was lower than 450 $\Omega\ \square^{-1}$. In particular, for the film with the sheet resistance of 150 $\Omega\ \square^{-1}$, nearly 20% differences were observed. This is because the conformational change to the linear structure of the PEDOT:PSS chain resulted in lower intrinsic resistance for the particles, so fewer PEDOT:PSS particles are required for the same sheet resistance.[17,41] As a result of the reduction in the number of PEDOT:PSS particles, the transmittance increases with the sheet resistance.

For the reasons stated above, the b* values (Fig. 6(b), right axis) were also lower for Na-removed PEDOT:PSS films.

The haziness (Fig. 6(b), left axis) of both Na-containing and Na-removed PEDOT:PSS films was lower than 0.4%, and slight increases were observed when sodium had been removed. Haziness is associated with the particle size. Since they show values lower than 0.5% immediately after synthesis, the properties of the films are applicable to electronic devices.

Colloidal stability of PEDOT:PSS dispersions

Colloidal stability, the ability of a dispersion to resist coagulation, is an important factor in processability. Since viscosity increases as particles coagulate, the colloidal stability was investigated through viscosity changes over time. Fig. 7 shows that the sodium-containing PEDOT:PSS dispersion exhibited very little variation in its viscosity over time, while the sodium-removed PEDOT:PSS dispersion displayed significant changes. The results show that residual sodium ions have a detrimental effect on the colloidal stability. This can be seen from the inset image in Fig. 7, which shows that particle coagulation had occurred after three months. This is because residual sodium ions affect the repulsion between two particles.[42–44] The excess PSS and its charge, which are located in the shell of PEDOT:PSS particles, cause repulsion between the particles so that they do not coagulate. As the sodium ion concentration is increased, the positive charges of the sodium ions compensate for the negative charges of PSS, and the repulsion is reduced. Consequently, particle aggregation occurs, and the particle size increases, leading to high viscosity.

Conclusions

In this study, we investigated the effects of metal ions, namely sodium ions, on the structure of PEDOT:PSS during polymerization and the resulting properties. The conformational structure change of PEDOT:PSS particles was investigated using XPS and Raman spectroscopy analyses. When sodium ions were removed, PSSNa segments were converted into PSSH. This led to a reduction in the coulombic interaction between PEDOT and PSS, which changed the conformational structure of the PEDOT:PSS chain from a coil to a linear structure. Furthermore, AFM analysis revealed that the residual sodium ions prevent the expansion of PEDOT grains by hindering phase separation. These structural changes induced the phase separation of PEDOT:PSS, enhancing the carrier mobility across the PEDOT chains. As a result, the electrical conductivity increased by approximately twice and the work function also increased from 5.04 to 5.39 eV. In addition, it was confirmed that the optical properties, namely the transmittance, haziness, and b* value, were improved. By comparing the optical properties with respect to the sheet resistance, we found that the improvement in the intrinsic properties of the particles decreased the amount of PEDOT required for the same sheet resistance. The viscosity changes over time showed that residual sodium ions in PEDOT:PSS dispersions had a significant effect on the colloidal stability, since they decrease the repulsion between the particles. Lastly, we analyzed the effects of the residual sodium ions in PEDOT:PSS dispersions and confirmed that the removal process is very important for application to organic electronic devices.

Conflicts of interest

There are no conflicts to declare.

Acknowledgements

This work was supported by the Nano Material Technology Development Program through the National Research Foundation of Korea (NRF) funded by the Ministry of Science, ICT & Future Planning (MSIP, Korea) (NRF-2014M3A7B4050960/2014M3A7B4051745). This research was supported by the Priority Research Centers Program through the National Research Foundation of Korea (NRF) funded by the Ministry of Education, Science and Technology (2009-0093823).

Notes and references

1 L. Carrasco–Valenzuela, E. A. Zaragoza–Contreras and A. Vega–Rios, *Polymer*, 2017, **130**, 124–134.
2 D. Yoo, J. Kim and J. H. Kim, *Nano Res.*, 2014, **7**, 717–730.
3 N. Terasawa and K. Asaka, *RSC Adv.*, 2018, **8**, 17732–17738.
4 W. Cho, S. Im, S. Kim, S. Kim and J. H. Kim, *Polymers*, 2016, **8**, 189.
5 C. Park, S. Im, W. Cho, Y. Kim and J. H. Kim, *RSC Adv.*, 2018, **8**, 12992–12998.
6 S. H. Kim, J. H. Kim, H. J. Choi and J. Park, *RSC Adv.*, 2015, **5**, 72387–72393.
7 D. Yoo, J. Kim, S. H. Lee, W. Cho, H. H. Choi, F. S. Kim and J. H. Kim, *J. Mater. Chem. A*, 2015, **3**, 6526–6533.
8 A. M. Nardes, M. Kemerink, M. De Kok, E. Vinken, K. Maturova and R. Janssen, *Org. Electron.*, 2008, **9**, 727–734.
9 W. Cho, J. K. Hong, J. J. Lee, S. Kim, S. Kim, S. Im, D. Yoo and J. H. Kim, *RSC Adv.*, 2016, **6**, 63296–63303.
10 J. Peng, X. Xu, C. Yao and L. Li, *RSC Adv.*, 2016, **6**, 100312–100317.
11 X. Li, Y. Hu, Z. Deng, L. Zhu, Y. Wang, D. Xu, Y. Hou and F. Teng, *Phys. Status Solidi A*, 2015, **212**, 1800–1804.
12 H. S. Dehsari, E. K. Shalamzari, J. N. Gavgani, F. A. Taromi and S. Ghanbary, *RSC Adv.*, 2014, **4**, 55067–55076.
13 J. Ouyang, *Displays*, 2013, **34**, 423–436.
14 C. Weijtens, V. Van Elsbergen, M. De Kok and S. De Winter, *Org. Electron.*, 2005, **6**, 97–104.
15 B. J. Worfolk, T. C. Hauger, K. D. Harris, D. A. Rider, J. A. Fordyce, S. Beaupré, M. Leclerc and J. M. Buriak, *Adv. Energy Mater.*, 2012, **2**, 361–368.
16 H. Park, S. H. Lee, F. S. Kim, H. H. Choi, I. W. Cheong and J. H. Kim, *J. Mater. Chem. A*, 2014, **2**, 6532–6539.
17 C. M. Palumbiny, J. Schlipf, A. Hexemer, C. Wang and P. Müller-Buschbaum, *Adv. Electron. Mater.*, 2016, **2**, 1500377.
18 C.-S. Chou, C.-S. Chou, Y.-T. Kuo and C.-P. Wang, *Adv. Powder Technol.*, 2013, **24**, 336–343.
19 T. Ji, L. Tan, X. Hu, Y. Dai and Y. Chen, *Phys. Chem. Chem. Phys.*, 2015, **17**, 4137–4145.
20 G. Greczynski, T. Kugler and W. Salaneck, *Thin Solid Films*, 1999, **354**, 129–135.
21 G. Greczynski, T. Kugler, M. Keil, W. Osikowicz, M. Fahlman and W. R. Salaneck, *J. Electron Spectrosc. Relat. Phenom.*, 2001, **121**, 1–17.
22 J. Hwang, F. Amy and A. Kahn, *Org. Electron.*, 2006, **7**, 387–396.
23 Z. Zhu, C. Liu, H. Shi, Q. Jiang, J. Xu, F. Jiang, J. Xiong and E. Liu, *J. Polym. Sci., Part B: Polym. Phys.*, 2015, **53**, 885–892.
24 M. Łapkowski and A. Proń, *Synth. Met.*, 2000, **110**, 79–83.
25 S. Garreau, G. Louarn, J. Buisson, G. Froyer and S. Lefrant, *Macromolecules*, 1999, **32**, 6807–6812.
26 S. Garreau, J. Duvail and G. Louarn, *Synth. Met.*, 2001, **125**, 325–329.
27 M. De Kok, M. Buechel, S. Vulto, P. Van de Weijer, E. Meulenkamp, S. De Winter, A. Mank, H. Vorstenbosch, C. Weijtens and V. Van Elsbergen, *Phys. Status Solidi A*, 2004, **201**, 1342–1359.
28 T.-C. Tsai, H.-C. Chang, C.-H. Chen, Y.-C. Huang and W.-T. Whang, *Org. Electron.*, 2014, **15**, 641–645.
29 J. Ouyang, Q. Xu, C.-W. Chu, Y. Yang, G. Li and J. Shinar, *Polymer*, 2004, **45**, 8443–8450.
30 S. H. Chang, C.-H. Chiang, F.-S. Kao, C.-L. Tien and C.-G. Wu, *IEEE Photonics J.*, 2014, **6**, 1–7.
31 Y. Xia, H. Zhang and J. Ouyang, *J. Mater. Chem.*, 2010, **20**, 9740–9747.
32 K. Sanglee, S. Chuangchote, P. Chaiwiwatworakul and P. Kumnorkaew, *J. Nanomater.*, 2017, **2017**, 8.
33 X. Crispin, F. Jakobsson, A. Crispin, P. Grim, P. Andersson, A. Volodin, C. Van Haesendonck, M. Van der Auweraer, W. R. Salaneck and M. Berggren, *Chem. Mater.*, 2006, **18**, 4354–4360.
34 C. Park, D. Yoo, J. J. Lee, H. H. Choi and J. H. Kim, *Org. Electron.*, 2016, **36**, 166–170.
35 Z. Yu, Y. Xia, D. Du and J. Ouyang, *ACS Appl. Mater. Interfaces*, 2016, **8**, 11629–11638.
36 Q. Wei, M. Mukaida, Y. Naitoh and T. Ishida, *Adv. Mater.*, 2013, **25**, 2831–2836.
37 I. Petsagkourakis, E. Pavlopoulou, E. Cloutet, Y. F. Chen, X. Liu, M. Fahlman, M. Berggren, X. Crispin, S. Dilhaire and G. Fleury, *Org. Electron.*, 2018, **52**, 335–341.
38 C. M. Palumbiny, J. Schlipf, A. Hexemer, C. Wang and P. Müller-Buschbaum, *Adv. Electron. Mater.*, 2016, **2**, 1500377.
39 S. Kim, B. Sanyoto, W. T. Park, S. Kim, S. Mandal, J. C. Lim, Y. Y. Noh and J. H. Kim, *Adv. Mater.*, 2016, **28**, 10149–10154.
40 T. W. Lee and Y. Chung, *Adv. Funct. Mater.*, 2008, **18**, 2246–2252.
41 N. Kim, S. Kee, S. H. Lee, B. H. Lee, Y. H. Kahng, Y. R. Jo, B. J. Kim and K. Lee, *Adv. Mater.*, 2014, **26**, 2268–2272.
42 Y. Mir, P. Auroy and L. Auvray, *Phys. rev. lett.*, 1995, **75**, 2863.
43 H. Dautzenberg, *Macromolecules*, 1997, **30**, 7810–7815.
44 K. Ogawa, S. Sato and E. Kokufuta, *Langmuir*, 2005, **21**, 4830–4836.